

This is the peer reviewed version of the following article:

***Efficient Electrochemical Water Oxidation by a Trinuclear Ru(bda) Macrocycle Immobilized on Multi-walled Carbon Nanotube Electrodes**, which has been published in final form at*

<https://onlinelibrary.wiley.com/doi/10.1002/aenm.202002329>

This article may be used for non-commercial purposes in accordance with Wiley Terms and Conditions for Self-Archiving." Copyright © 1999-2020 John Wiley & Sons, Inc

Formatted: Font: Italic

Formatted: Justified, Space After: 0 pt

Formatted: Hyperlink, Font: 11 pt, Not Bold, German (Germany)

Formatted: Font: (Default) +Body (Calibri), 12 pt, Bold, Not Italic

Field Code Changed

Formatted: English (United Kingdom)

Efficient Electrochemical Water Oxidation by a Trinuclear Ru(bda) Macrocycle Immobilized on Multi-walled Carbon Nanotube Electrodes

Dorothee Schindler, Marcos Gil-Sepulcre, Joachim O. Lindner, Vladimir Stepanenko, Dooshaye Moonshiram, Antoni Llobet* and Frank Würthner*

Abstract: Catalytic water splitting is a viable process for the generation of renewable fuels. Here we report for the first time that a trinuclear supramolecular Ru(bda) (bda: 2,2'-bipyridine-6,6'-dicarboxylic acid) catalyst, anchored on multi-walled carbon nanotubes (MWCNTs) and subsequently immobilized on glassy carbon electrodes, shows outstanding performance in heterogeneous water oxidation. Activation of the catalyst on anodes by repetitive cyclic voltammetry (CV) scans resulted in a very high catalytic current density of 186 mA/cm² at a potential of 1.45 V vs NHE. The remarkably high stability of the hybrid anode was demonstrated by XAS spectroscopy and electrochemically revealing the absence of any degradation after 1.8 million turnovers. Foot of the wave analysis (FOWA) of CV data of activated electrodes with different concentrations of catalyst indicated a monomolecular water nucleophilic attack (WNA) mechanism with an apparent rate constant of TOF_{max} (turnover frequency) of 3200 s⁻¹.

Commented [MGS1]: I would not put "very high" in the abstract

"...scans resulted in a catalytic current density of 186 mA/cm² at a potential of 1.45 V vs NHE..."

D. Schindler, Dr. V. Stepanenko, Prof. Dr. F. Würthner*
Universität Würzburg, Institut für Organische Chemie, Am Hubland, 97074 Würzburg (Germany)
E-mail: wuerthner@uni-wuerzburg.de

Dr. J. O. Lindner, Dr. V. Stepanenko, Prof. Dr. F. Würthner*
Center for Nanosystems Chemistry, Theodor-Boveri-Weg, 97074 Würzburg (Germany)

Dr. M. Gil-Sepulcre, Prof. Dr. A. Llobet*
Institut Català d'Investigació Química (ICIQ), Barcelona Institute of Science and Technology (BIST)
Avinguda Països Catalans 16, 43007 Tarragona (Spain)
E-mail: allobet@iciq.cat

Prof. Dr. A. Llobet*

Departament de Química, Universitat Autònoma de Barcelona, Cerdanyola del Vallès, 08193 Barcelona (Spain)

Dr. D. Moonshiram

Instituto Madrileño de Estudios Avanzados en Nanociencia (IMDEA Nanociencia)
Calle Faraday, 9, 28049 Madrid (Spain)

Natural photosynthesis has inspired in the last decades many novel approaches for the generation of renewable fuels.^[1-6] In this regard, catalytic water splitting into molecular oxygen and hydrogen ~~appears~~ is a highly promising process.^[7-11] Toward this goal, however, efficient water oxidation catalysts (WOCs) are required to overcome the high energy barriers of the demanding anodic half reaction of water oxidation into molecular oxygen.^[12-14] Indeed, considerable progress has been made over the last decades in the development of molecular WOCs and valuable mechanistic understanding of catalytic water oxidation has been acquired.^[15-17] In particular, the class of molecular Ru(bda) catalysts (bda: 2,2'-bipyridine-6,6'-dicarboxylic acid) has shown high catalytic efficiencies comparable to nature's oxygen evolving complex.^[16, 18] However, for the implementation of such WOCs in water splitting devices their immobilization on proper surfaces is required.^[19-20]

For the immobilization of homogeneous WOCs onto electrodes, mainly two strategies have been employed. One of them is based on covalent attachment of molecular catalysts to electrode surfaces by silane-, carboxylate- or phosphonate-functionalized ligands.^[21-26] Another approach is a supramolecular one, comprising introduction of aromatic groups to the WOCs to facilitate non-covalent π - π interactions between the catalyst and a supporting material like carbon nanotubes (CNTs).^[27-28] Due to their large surface area as well as high conductivity and stability,^[29-32] CNTs are properly suited for immobilization of catalysts on electrodes. Indeed, Sun and coworkers have shown that a Ru(bda)(pic)₂ WOC, containing axial pyridyl ligands that are functionalized with pyrene groups through amide linkers, can be immobilized on multi-walled carbon nanotubes (MWCNTs).^[27] Recently, ~~also~~ some of us have also successfully anchored a Ru(tda) (tda: [2,2':6',2''-terpyridine]-6,6''-dicarboxylic acid) catalyst bearing pyrene-functionalized axial ligands on MWCNTs by π - π interactions and demonstrated heterogeneous water oxidation for this hybrid material.^[28] It has been reported in literature that immobilization of molecular Ru(bda) catalysts, which operate by I2M (interaction of two M-O units) mechanism^[33] in homogeneous phase on electrodes, leads to adverse effects on their catalytic activity in heterogeneous catalysis^[34-35] due to restricted mobility, associated with a switch to the WNA (water nucleophilic attack) mechanism.^[33] This implies that Ru-based WOCs functioning through the latter mechanism are favorable for heterogeneous catalysis.^[36-37]

Commented [MGS2]: [2,2'-bipyridine]-6,6'-dicarboxylate, right??

Once it is coordinated, it is deprotonated

Commented [MGS3]: This is not exactly pic, right?

"Indeed, Sun and coworkers have shown that a **derivative of** Ru(bda)(pic)₂ WOC, containing axial pyridyl ligands that are functionalized with pyrene groups through amide linkers"

Or

"Indeed, Sun and coworkers have shown that a **Ru(bda)** WOC, containing axial pyridyl ligands that are functionalized with pyrene groups through amide linkers"

Commented [MGS4]: Same comment

The "tda" is not protonated:

Thus, we envisioned that macrocyclic WOCs bearing three Ru(bda) units such as **MC3** (for structure see Fig. 1a) should be a promising candidate for heterogeneous water oxidation as **MC3** exhibits high catalytic efficiency in homogeneous water oxidation via a WNA mechanism^[38-39] and benefits from the supramolecular arrangement.^[40] As this metallomacrocyclic complex comprises three linear aromatic linker ligands in addition to the three bda units, we assumed that it should be possible to anchor this catalyst on CNTs by non-covalent π - π and CH- π interactions towards the graphene-like surface without further functionalization for heterogeneous catalytic water oxidation.^[41] Here we report that **MC3** indeed adheres to CNTs as confirmed by electrochemical techniques and atomic force microscopy (AFM). More importantly, CNT-anchored **MC3** immobilized on glassy carbon electrodes performed outstanding catalytic activity in electrochemically driven water oxidation underlining its potential for device application.

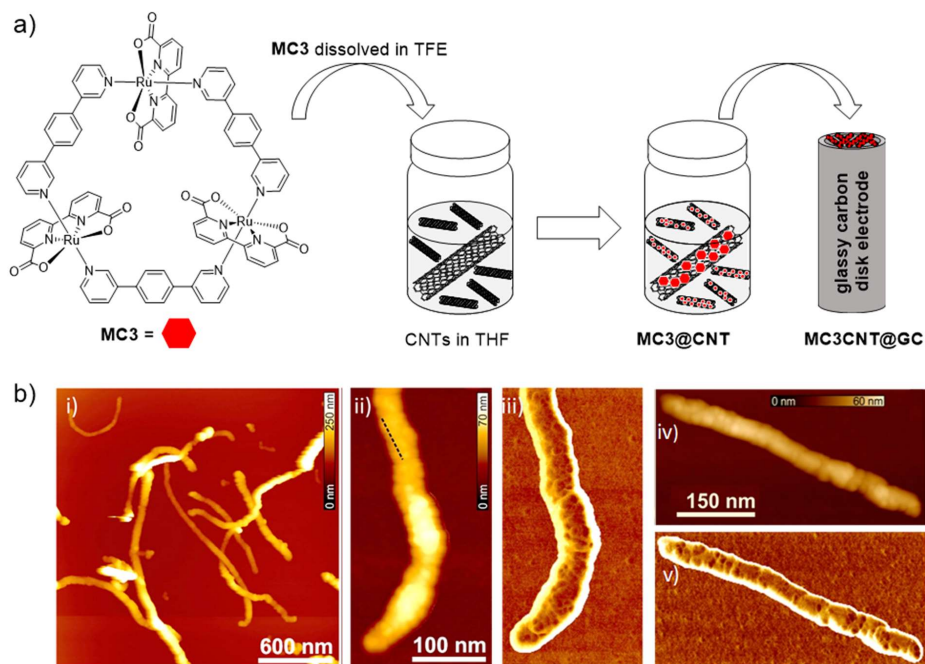


Figure 1: a) Structure of the Ru(bda) macrocycle **MC3** and schematic illustration of its immobilization on CNTs and subsequent deposition onto a glassy carbon disk. b) Height (i, ii, iv) and phase (iii, v) AFM images obtained after spin-coating a dispersion of **MC3@CNT** (0.2 mL of **MC3** in TFE ($c = 1$ mg/mL) in 1 mL of MWCNTs in THF ($c = 1$ mg/mL)) onto a silicon wafer. Z scale: 250 nm (i), 70 nm (ii) and 60 nm (iv). Images in iii and v show one single magnified nanotube, respectively, decorated with **MC3** molecules.

To anchor trinuclear Ru(bda) catalyst **MC3** on MWCNT surface, 0.1 mL of a solution of **MC3** in trifluoroethanol (TFE) was added to a freshly prepared dispersion of MWCNTs in THF (Fig. 1a). Immediate decolourization of the mixture indicated the binding of the catalyst onto the surface of the CNTs. To confirm that catalyst **MC3** is indeed attached to the CNTs, AFM measurements were

Commented [D5]: If you submit to Angew. Chem. It is perhaps best to homogenize to british english , otherwise it is absolutely fine.

performed by spin-coating a dispersion of **MC3@CNT** onto a silicon wafer (Fig. 1b). Magnification of one single CNT (Fig. 1b, ii-v) clearly shows the distribution of the anchored **MC3** molecules on the nanotube surface. Thus, for the first time we could proof-prove by a microscopic method direct anchoring of an unfunctionalized Ru(bda) complex to CNTs through non-covalent interactions.

For electrochemical studies, working electrodes (WE) were prepared by drop-casting a suspension of **MC3@CNT** onto glassy carbon disk electrodes ($S = 0.07 \text{ cm}^2$, denoted as **MC3@CNT@GC**). Cyclic voltammetry (CV) experiments were then performed with these electrodes in a 1 M phosphate buffer solution (pH 7) using a three electrode cell. A platinum mesh and Hg/HgSO₄ electrode were used as counter (CE) and reference electrodes (RE), respectively. All potentials reported hereinafter are converted and referenced to NHE. The catalytic process was initiated at an onset potential of 1.05 V (Fig. S1) and current densities of about 50 mA/cm² at $E = 1.45 \text{ V}$ were observed in the first cycle (Fig. 2d, black line). Repetitive CV cycles up to a potential of 1.35 V revealed a steady rise of the catalytic current (Fig. 2a, b), along with changes in the non-catalytically active redox waves (Fig. 2a, inset). As the number of CV cycles increases, higher catalytic current densities are observed until a plateau is reached after around 100 cycles (Fig. 2b).

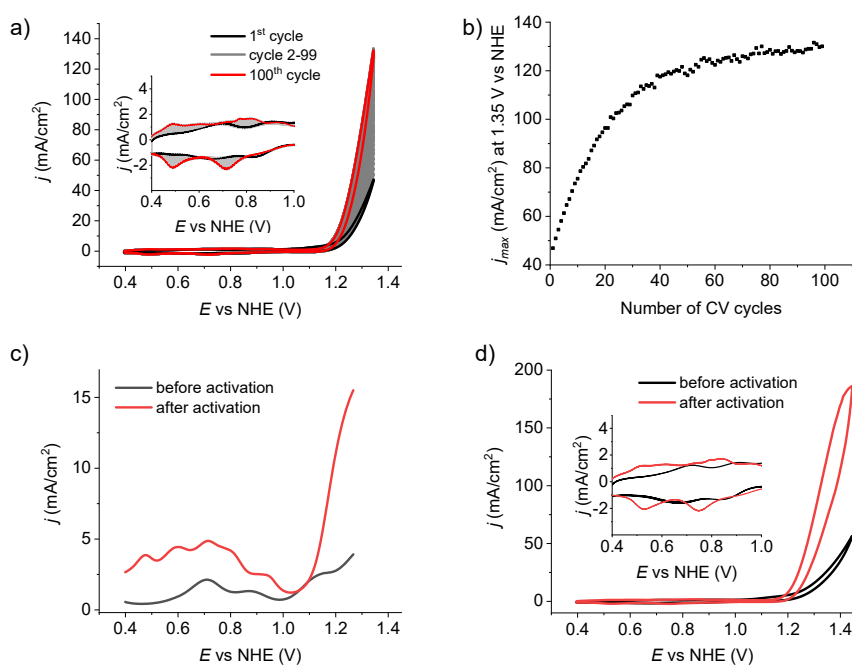


Figure 2: Electrochemical experiments with **MC3@CNT@GC** in 1 M phosphate buffer (pH 7). a) 100 repetitive CV scans (scan rate: 100 mV/s). Inset: Enlarged area of the non-catalytic waves. Initial species in the first cycle is shown in black, 100th cycle is shown in red. Scans 2-99 are depicted in grey. b) Development of the maximal current densities at $E = 1.35 \text{ V}$ vs NHE with the increasing number of CV scans. c) Comparison of the differential pulse voltammograms of the initial species (black line)

and the final species after 100 CV cycles (red line). d) Comparison of the cyclic voltammograms (scan rate: 100 mV/s) of the initial (black line) and the final species (red line) after 100 CV cycles.

Control CV experiments confirmed that CNT decorated electrode without the catalyst- (**CNT@GC**, Fig. S2a, blank) does not produce any significant current under identical experimental conditions. Interestingly, **MC3** as a homogeneous catalyst in a phosphate buffer/TFE 1:1 mixture (pH 7) does not show any comparable catalytic activity in water oxidation (Fig. S2b). Investigations of the redox properties of homogeneous **MC3** by differential pulse voltammetry (DPV) showed three reversible oxidation processes that are assignable to the transitions from the Ru^{II} to Ru^V oxidation states.^[38] DPV analysis of **MC3@CNT@GC** electrode revealed that the first and the second oxidation waves of immobilized **MC3** correspond to the Ru^{III/II} and Ru^{IV/III} redox couples at $E = 0.68$ V and 0.85 V, respectively, and are not influenced by the immobilization of the catalyst. The Ru^{V/IV} oxidation is shifted to higher potentials from 1.02 V to 1.11 V in the case of **MC3@CNT@GC** compared to the non-immobilized catalyst (Fig. S2c, d).

By DPV analysis, the appearance of additional redox waves of **MC3@CNT@GC** and a rise in the catalytic current can be observed after the final state is reached upon 100 CV cycles (Fig. 2c). This indicates the formation of a new and even more active species on the electrode. Five redox processes can be seen before the onset of the water oxidation catalysis, which is now shifted to higher potentials and appears at $E_{onset} = 1.15$ V. The Ru^{V/IV} oxidation of the initial species is covered by the catalytic slope of the newly formed species and, therefore, not observable any more. The first redox process of the newly formed species arises at 0.50 V, which presumably corresponds to the Ru^{III/II} redox process and is also shifted to lower potentials than in the initial species. Similar electrochemical activation processes have already been described for other Ru catalysts like Ru(tda)(py)₂ (tda = [2,2':6',2''-terpyridine]-6,6''-dicarboxylic acid) or Ru(pdc)(bpy)₂ (pdc: pyridyl-2,6-dicarboxylic acid),^[17, 42] where the formation of a Ru aqua species as active catalyst was supposed after repetitive CV cycles. However, such activated species has not been reported for Ru(bda) catalysts. XAS spectroscopy provides further evidence of the molecularity of the water oxidation active catalyst since no RuO₂ can be detected at the surface of the electrode after catalysis (Fig. S3, Table S1-S3).

After removing all oxygen bubbles from the surface of the activated electrodes (**act-MC3@CNT@GC**), ~~one~~ a cyclic voltammogram was recorded and compared to the one of the unactivated electrode (**MC3@CNT@GC**, Fig. 2d). An exceptionally high current density (j) of 186 mA/cm² was reached at $E = 1.45$ V after the activation process, which is about four times higher than the value observed before activation (Fig. 2d, average in three independent experiments: 176 mA/cm², Fig. S4). Earlier approaches by Sun and coworkers of immobilizing pyrene-functionalized Ru(bda) catalysts on an ITO surface using carbon nanotubes as support resulted in current densities of only 720 μ A/cm².^[27] Thus,

the observed j_{max} value for anchored and activated **MC3** is the highest one reported so far for Ru(bda) catalysts with **proved/confirmed** molecular active species and comparable with the very recently observed maximum current density of 240 mA/cm² for an immobilized Ru(tda) oligomer.^[41]

Commented [D6]: Proved is used again in the next sentence.

Proven to be highly efficient, the stability and efficiency of the **act-MC3@CNT@GC** electrodes was then investigated by controlled potential electrolysis (CPE) experiments (Fig. 3). A two-compartment setup was used, where the working and the reference electrodes were placed in one chamber and the counter electrode in the other one. A constant potential of 1.6 V was applied. **Almost** no decrease in the catalytic current during 6 hours confirms that the immobilized catalyst does not undergo any considerable degradation or detachment from the electrode during continuous catalytic water oxidation process (Fig. 3a). With only a negligible loss, 97 % of the initial current density **is still remains remained** after 6 hours. No significant changes in the CV were observed before and after this experiment, confirming the high stability of the activated species (Fig. S5a).

Commented [MGS7]: I don't see any decrease either in the CPE or CVs before and after. I would eliminate "Almost"

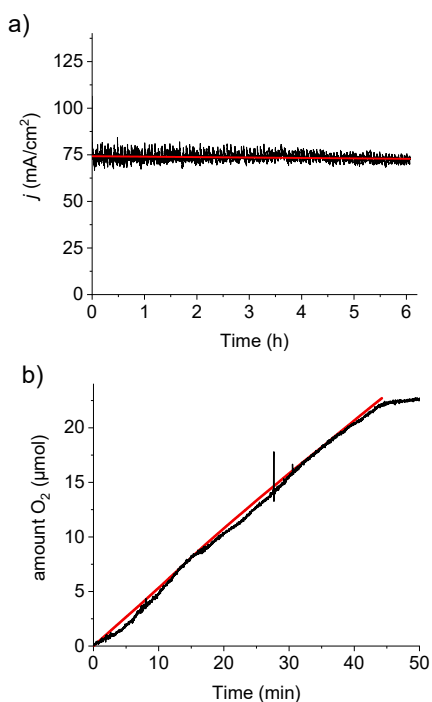


Figure 3: a) Controlled potential electrolysis (CPE) experiment of activated electrode **act-MC3@CNT@GC** in a 1 M phosphate buffer (pH 7) at 1.6 V vs NHE for 6 h. b) Determination of the Faraday efficiency. The red line shows the theoretical amount of produced oxygen calculated from the passed charge in a CPE experiment assuming a Faraday efficiency of 100 %. The black line corresponds to the head-space analysis of the amount of oxygen detected by a Clark electrode.

Assuming that all electrons passing through the system are involved in the catalytic reaction, the amount of generated oxygen can be calculated from the charge after 6 hours (Fig. S5b). According to

the water oxidation reaction and assuming 100 % Faraday efficiency (which will be confirmed below), four electrons are used to generate one molecule of oxygen. Therefore, the amount of generated oxygen was calculated from the passed charge by employing Faraday law to be $2.6 \cdot 10^{-4}$ mol and divided by the total amount of Ru-centers after activation ($1.44 \cdot 10^{-10}$ mol) on the electrode. The details for this determination are given in the SI (Fig. S5 – S6 and description given under Fig. S6). These values lead to a remarkably high turnover number (TON) of 1.8 million referred to activated Ru on the electrode (0.5 million with respect to the total amount of Ru on the electrode before activation (Fig S6, d)). Assigning the first oxidation process in the CV after activation to the one-electron transfer process of the Ru^{III/II} oxidation in every Ru(bda) center of the trinuclear Ru(bda) complex **MC3**, the amount of Ru on the surface of the **act-MC3@CNT@GC** electrode can be determined by integrating the area under the respective waves in the cathodic and anodic scan (Fig. S6 a-c).

To verify that no side processes other than water oxidation take place during this electrochemical reaction and all electrons are involved in the water oxidation, the Faraday efficiency of **act-MC3@CNT@GC** was determined. The amount of charge passing through the system was recorded by the potentiostat and the actual amount of oxygen produced during one CPE experiment was measured by a gas phase Clark electrode in the head-space of the chamber containing the working electrode. For this purpose, a glassy carbon plate was used as a working electrode due to its increased surface area. A constant potential of 1.3 V was applied, and after few seconds bubbles of oxygen could be seen by the naked eye on the working electrode. The CPE experiment was stopped after 45 minutes. The quantity of detected oxygen was compared to the theoretical maximum calculated [one](#) assuming a Faraday efficiency of 100 % (for details see Methods in SI). Almost no deviations between these values (Fig. 3b) imply a Faraday efficiency of 99 %.

The foot of the wave analysis (FOWA), first developed by Savéant and coworkers^[43] and applied for electrocatalytic reduction processes^[44-48] and later adapted to the electrochemical water oxidation,^[36] was performed to [gain](#) more insights into the kinetics of the electrocatalytic water oxidation reaction performed by **act-MC3@CNT@GC** (Fig. 4). Electrodes with different concentrations of the catalyst were prepared, activated and subsequently CV experiments were performed (Fig. 4a, Fig. S7) in order to apply the FOWA methodology.

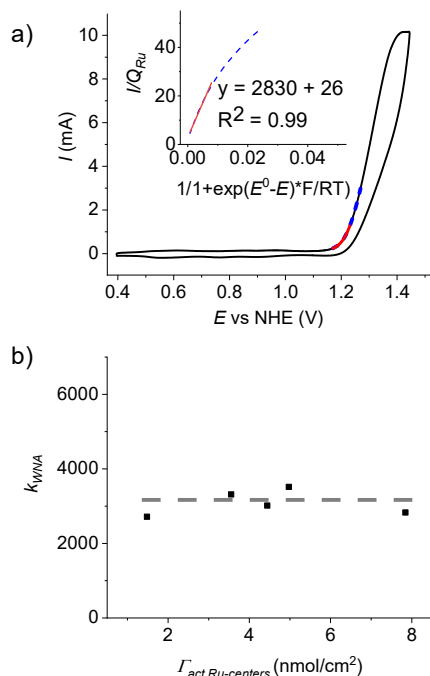


Figure 4: a) The solid black line shows the second cycle of the CV of **act-MC3@CNT@GC** in a 1 M phosphate buffer (pH 7) for a surface concentration of the active species of $\Gamma_{act,cat} = 5.3 \text{ nmol/cm}^2$. The region used for the FOWA is indicated by the blue dotted line. The red solid line at the foot of the wave shows the area which is used for the determination of the apparent rate constant. Inset: i/Q_{Ru} vs $1/(1+\exp(E^0-E)*F/RT)$ plot assuming a WNA mechanism for the immobilized macrocyclic catalyst. The apparent rate constant k_{WNA} at the foot of the wave was obtained by fitting the points represented by the solid red line. b) The k_{WNA} values obtained from i/Q_{Ru} vs $1/(1+\exp(E^0-E)*F/RT)$ plot (a, inset) at the corresponding surface concentrations of the active species are shown as black data points. Independence of the k_{WNA} values of the surface concentration indicated by the grey dashed line is in agreement with the assumption of a WNA mechanism on the surface.

For the extraction of the kinetic data, the first data points of the catalytic slope of one CV cycle (Fig. 4a, blue dots) were used. The charge corresponding to one Ru oxidation event (Q_{Ru}) was determined by integration of the area under the wave corresponding to the $\text{Ru}^{III/II}$ oxidation process of the active species (Fig. S6). By assuming a hetero-WNA mechanism taking place on the electrode^s surface, these data points were plotted according to i/Q_{Ru} vs $1/(1+\exp(E^0-E)*F/RT)$ (Fig. 4a, inset; for details see Methods in SI and equation [S1]). The gradient of the received curve was fitted by linear regression (Fig. 4a, inset; red line). Its slope represents the apparent pseudo-rate constant (k_{WNA} value) at the foot of the catalytic wave for each electrode with different catalyst concentrations, which equals the TOF_{max} value (see Methods in SI and equation [S2]). The independence of k_{WNA} values versus surface concentration of the activated Ru-centers (Fig. 4b) is a clear indication of a single mechanism operating in this system. Further, the first-order kinetics with regards to the catalyst's concentration agrees with a WNA mechanism taking place for **act-MC3@CNT@GC**. An average apparent rate constant of $k_{WNA} = \text{TOF}_{max} = (3197 \pm 395) \text{ s}^{-1}$ was obtained (Fig. 4b). It has been reported in literature that a $\text{Ru}(\text{bda})(\text{L})_2$ catalyst (L = functionalized pyridine ligand), which oxidizes water via a bimolecular I2M O-O bond

Commented [MGS8]: It would be much correct to mention "loading" instead of "concentration"

Commented [MGS9]: Do we have a CV (Fig. 4) that is closer to the averaged value for Figure 4??

formation step in homogeneous catalysis, not only drops in activity, when immobilized on an electrode surface changing to a WNA mechanism (FOWA: $\text{TOF}_{\text{max}} = 53 \text{ s}^{-1}$ homogeneous; $\text{TOF}_{\text{max}} = 1.9 \text{ s}^{-1}$ heterogeneous), but also ends up with decomposing to RuO_2 .^[34-36] In contrast, a $\text{Ru}(\text{tda})(\text{L})_2$ catalyst which functions through a WNA mechanism in homogeneous catalysis does not undergo any significant change upon immobilization (FOWA: $\text{TOF}_{\text{max}} = 8000 \text{ s}^{-1}$ homogeneous; $\text{TOF}_{\text{max}} = 9000 \text{ s}^{-1}$ heterogeneous).^[28, 34] The latter is also the case for our trinuclear $\text{Ru}(\text{bda})$ macrocycle **MC3**, which was previously reported to function through a WNA mechanism.^[38] Since activation of **MC3** is only observed upon its adsorption on MWCNTs, the strength of non-covalent interactions with the CNT surface is assumed to play a crucial role during this process. Indeed, our semiempirical calculations using graphene-like surface as a model indicated that a structure with partial decoordination of bda ligands, allowing for the coordination of additional water molecules to Ru (Fig. 5), introduces additional stabilizing π - π interactions compared to different possible conformations of **MC3** (Fig. S8). Such diaqua species would explain the observed, notably changed redox behavior of **act-MC3@CNT@GC** compared to the non-activated **MC3@CNT@GC** and may play a role in electrochemical heterogeneous water oxidation by $\text{Ru}(\text{bda})$ macrocycle.

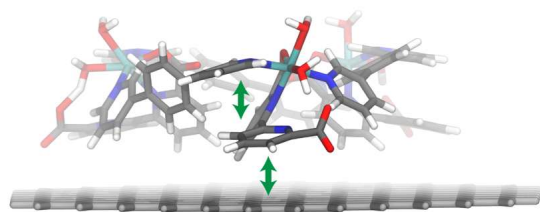


Figure 5: Optimized structure based on semiempirical calculations of the proposed activated species **act-MC3@CNT@GC** (grey: carbon, white: hydrogen, blue: nitrogen, red: oxygen, turquoise: ruthenium). A hexagonal graphene sheet has been used as a model for the graphitic surface of MWCNTs. For computational details, see Methods in SI. Green double-headed arrows indicate attractive π - π interactions.

In conclusion, we have successfully immobilized our macrocyclic **MC3** catalyst onto CNTs as confirmed by electrochemical techniques and AFM images. Taking advantage of the intrinsic properties of CNTs, glassy carbon electrodes with anchored **MC3** catalyst were prepared. To the best of our knowledge, this is the first report of an electrochemical activation of a $\text{Ru}(\text{bda})$ complex that has been transformed into a more active species by repetitive CV cycles. A current density as high as 186 mA/cm^2 was observed, which is among the highest values reported so far for molecular Ru catalysts anchored on solid state anodes. A Faraday efficiency of 99 % together with XAS spectroscopy demonstrates that the activated species does not undergo any unproductive side reactions during the catalytic process and neither the formation of RuO_2 . With a remarkably high TON value of 1.8 million and a TOF_{max} of 3200 s^{-1} the **act-MC3@CNT@GC** electrodes are efficient devices for electrochemically driven heterogeneous water oxidation.

Acknowledgements

This project has received funding from the European Research Council (ERC) under the European Union's Horizon 2020 research and innovation programme (grant agreement No. 787937). We thank the Alexander von Humboldt foundation for supporting this collaborative research with a Humboldt research award for A. L. Hobet. A. L. also acknowledges support from [Ministerio de Ciencia e Innovación, FEDER and AGAUR through grants: PID2019-111617RB-I00 and 2017-SGR-163](#). D.M acknowledges funding from the Severo Ochoa Excellence program from the Instituto IMDEA Nanociencia, ~~and~~ the Acciones de Dinamización "Europa Investigacion" grant (EIN2019-103399) ~~and~~ the Spanish [Ministerio de Ciencia, Innovacion y Universidades grant \(PID2019-111086RA-I00\)](#). This research used resources of the Advanced Photon Source (Beamline 9 BM-B), an Office of Science User Facility operated for the U.S. Department of Energy (DOE) Office of Science by Argonne National Laboratory, and was supported by the U.S. DOE under Contract No. DE-AC02-06CH11357, ~~and the Canadian Light Source and its funding partners.~~

Keywords: electrocatalysis • heterogeneous water oxidation • renewable fuels • ruthenium bda complexes • WOCs

Formatted: Font: 9 pt

References

- [1] P. D. Frischmann, K. Mahata, F. Würthner, *Chem. Soc. Rev.* **2013**, *42*, 1847-1870.
- [2] S. Berardi, S. Drouet, L. Francas, C. Gimbert-Surinach, M. Guttentag, C. Richmond, T. Stoll, A. Llobet, *Chem. Soc. Rev.* **2014**, *43*, 7501-7519.
- [3] B. Zhang, L. Sun, *Chem. Soc. Rev.* **2019**, *48*, 2216-2264.
- [4] M. G. Walter, E. L. Warren, J. R. McKone, S. W. Boettcher, Q. Mi, E. A. Santori, N. S. Lewis, *Chem. Rev.* **2010**, *110*, 6446-6473.
- [5] R. J. Detz, K. Sakai, L. Spiccia, G. W. Brudvig, L. Sun, J. N. H. Reek, *ChemPlusChem* **2016**, *81*, 1024-1027.
- [6] T. Sharifi, C. Larsen, J. Wang, W. L. Kwong, E. Gracia-Espino, G. Mercier, J. Messinger, T. Wågberg, L. Edman, *Adv. Energy Mater.* **2016**, *6*, 1600738.
- [7] M. Beller, G. Centi, L. Sun, *ChemSusChem* **2017**, *10*, 6-13.
- [8] *Molecular Water Oxidation Catalysis: A Key Topic for New Sustainable Energy Conversion Schemes* Llobet, A., Ed.; John Wiley and Sons Ltd., 2014.
- [9] J. O. M. Bockris, *Materials* **2011**, *4*, 2073-2091.
- [10] J. Qi, W. Zhang, R. Cao, *Adv. Energy Mater.* **2018**, *8*, 1701620.
- [11] J. R. McKone, N. S. Lewis, H. B. Gray, *Chem. Mater.* **2014**, *26*, 407-414.
- [12] J. Hessels, R. J. Detz, M. T. M. Koper, J. N. H. Reek, *Chem. Eur. J.* **2017**, *23*, 16413-16418.
- [13] A. Kudo, Y. Miseki, *Chem. Soc. Rev.* **2009**, *38*, 253-278.
- [14] S. Ye, C. Ding, M. Liu, A. Wang, Q. Huang, C. Li, *Adv. Mater.* **2019**, *31*, 1902069.
- [15] D. Moonshiram, V. Purohit, J. J. Concepcion, T. J. Meyer, Y. Pushkar, *Materials* **2013**, *6*, 392-409.
- [16] B. Zhang, L. Sun, *J. Am. Chem. Soc.* **2019**, *141*, 5565-5580.
- [17] M. A. Hoque, J. Benet-Buchholz, A. Llobet, C. Gimbert-Suriñach, *ChemSusChem* **2019**, *12*, 1949-1957.
- [18] L. Duan, F. Bozoglian, S. Mandal, B. Stewart, T. Privalov, A. Llobet, L. Sun, *Nat. Chem.* **2012**, *4*, 418-423.
- [19] R. Brimblecombe, G. C. Dismukes, G. F. Swiegers, L. Spiccia, *Dalton Trans.* **2009**, *43*, 9374-9384.
- [20] Z. Chen, J. J. Concepcion, J. W. Jurss, T. J. Meyer, *J. Am. Chem. Soc.* **2009**, *131*, 15580-15581.
- [21] Y. Gao, X. Ding, J. Liu, L. Wang, Z. Lu, L. Li, L. Sun, *J. Am. Chem. Soc.* **2013**, *135*, 4219-4222.
- [22] M. Yamamoto, Y. Nishizawa, P. Chabera, F. Li, T. Pascher, V. Sundstrom, L. Sun, H. Imahori, *Chem. Commun.* **2016**, *52*, 13702-13705.
- [23] L. Zhang, Y. Gao, X. Ding, Z. Yu, L. Sun, *ChemSusChem* **2014**, *7*, 2801-2804.
- [24] F. Li, K. Fan, L. Wang, Q. Daniel, L. Duan, L. Sun, *ACS Catal.* **2015**, *5*, 3786-3790.
- [25] F. L. Ke Fan, Lei Wang, Q. Daniel, E. Gabrielsson, L. Sun, *Phys. Chem. Chem. Phys.* **2014**, *16*, 25234 - 25240.
- [26] J. Odrobina, J. Scholz, M. Risch, S. Dechert, C. Jooss, F. Meyer, *ACS Catal.* **2017**, *7*, 6235-6244.
- [27] F. Li, B. Zhang, X. Li, Y. Jiang, L. Chen, Y. Li, L. Sun, *Angew. Chem. Int. Ed.* **2011**, *50*, 12276-12279; *Angew. Chem.* **2011**, *123*, 12484-12487.
- [28] J. Creus, R. Matheu, I. Peñafiel, D. Moonshiram, P. Blondeau, J. Benet-Buchholz, J. García-Antón, X. Sala, C. Godard, A. Llobet, *Angew. Chem. Int. Ed.* **2016**, *55*, 15382-15386; *Angew. Chem.* **2016**, *128*, 15608-15612.
- [29] N. Karousis, N. Tagmatarchis, D. Tasis, *Chem. Rev.* **2010**, *110*, 5366-5397.
- [30] V. Strauss, A. Roth, M. Sekita, D. M. Guldi, *Chem* **2016**, *1*, 531-556.
- [31] V. Sgobba, D. M. Guldi, *Chem. Soc. Rev.* **2009**, *38*, 165-184.
- [32] T. Umeyama, H. Imahori, *Energy Environ. Sci.* **2008**, *1*, 120-133.
- [33] X. Sala, S. Maji, R. Bofill, J. García-Antón, L. Escriche, A. Llobet, *Acc. Chem. Res.* **2014**, *47*, 504-516.
- [34] P. Garrido-Barros, R. Matheu, C. Gimbert-Suriñach, A. Llobet, *Curr. Opin. Electrochem.* **2019**, *15*, 140-147.
- [35] R. Matheu, L. Francàs, P. Chernev, M. Z. Ertem, V. Batista, M. Haumann, X. Sala, A. Llobet, *ACS Catal.* **2015**, *5*, 3422-3429.

Formatted: Spanish (Spain)

- [36] R. Matheu, S. Neudeck, F. Meyer, X. Sala, A. Llobet, *ChemSusChem* **2016**, *9*, 3361-3369.
- [37] D. W. Shaffer, Y. Xie, J. J. Concepcion, *Chem. Soc. Rev.* **2017**, *46*, 6170-6193.
- [38] M. Schulze, V. Kunz, P. D. Frischmann, F. Würthner, *Nat. Chem.* **2016**, *8*, 576-583.
- [39] V. Kunz, D. Schmidt, M. I. S. Röhr, R. Mitrić, F. Würthner, *Adv. Energy Mater.* **2017**, *7*, 1602939.
- [40] V. Kunz, J. O. Lindner, M. Schulze, M. I. S. Rohr, D. Schmidt, R. Mitric, F. Würthner, *Energy Environ. Sci.* **2017**, *10*, 2137-2153.
- [41] [Md. A. Hoque, M. Gil-Sepulcre, A. de Aguirre, J. A. A. W. Elemans, D. Moonshiram, R. Matheu, Y. Shi, J. Benet-Buchholz, X. Sala, M. Malfois, E. Solano, J. Lim, A. Garzón-Manjón, C. Scheu, M. Lanza, F. Maseras, C. Gimbert-Suriñach and A. Llobet, *Nat. Chem.* **2020**, in press. DOI: \[XXXXXXXXXX\]\(#\)](#), [A. Llobet, unpublished results 2019.](#)
- [42] R. Matheu, M. Z. Ertem, J. Benet-Buchholz, E. Coronado, V. S. Batista, X. Sala, A. Llobet, *J. Am. Chem. Soc.* **2015**, *137*, 10786-10795.
- [43] C. Costentin, S. Drouet, M. Robert, J.-M. Savéant, *J. Am. Chem. Soc.* **2012**, *134*, 11235-11242.
- [44] C. Costentin, S. Drouet, M. Robert, J.-M. Savéant, *Science* **2012**, *338*, 90-94.
- [45] V. Artero, J.-M. Savéant, *Energy Environ. Sci.* **2014**, *7*, 3808-3814.
- [46] C. Costentin, J.-M. Savéant, *ChemElectroChem* **2014**, *1*, 1226-1236.
- [47] C. Costentin, H. Dridi, J.-M. Savéant, *J. Am. Chem. Soc.* **2014**, *136*, 13727-13734.
- [48] C. Costentin, G. Passard, J.-M. Savéant, *J. Am. Chem. Soc.* **2015**, *137*, 5461-5467.

Formatted: German (Germany)

Commented [AL10]: They are ridiculously slow. It was formally accepted on June 16th!!

Formatted: Font: Bold